

Structural analysis of heat-treated birch (*Betula papyrifera*) surface during artificial weathering

Xianai Huang^a, Duygu Kocaefe^{*a}, Yasar Kocaefe^a, Yaman Boluk^b, Cornélia Krause^a

^aUniversité du Québec à Chicoutimi, Canada
555, boul. de l'Université, Chicoutimi Québec Canada G7H 2B1

^bUniversity of Alberta, Canada
3-142 Markin/CNRL Natural Resources Engineering Facility
Edmonton, Alberta, Canada T6G 2W2

Corresponding author:

Duygu Kocaefe
E-mail: dkocaefe@uqac.ca
Phone: 418-545 5011 ext.5215
Fax: 418-545-5012

Abstract

Effect of artificial weathering on the surface structural changes of birch (*Betula papyrifera*) wood, heat-treated to different temperatures, was studied using the fluorescence microscopy and the scanning electron microscopy (SEM). Changes in the chemical structure of wood components were analyzed by FTIR in order to understand the mechanism of degradation taking place due to heat treatment and artificial weathering. The results are compared with those of the untreated (kiln-dried) birch. The SEM analysis results show that the effect of weathering on the cell wall of the untreated birch surface is more than that of heat-treated samples. The FTIR spectroscopy results indicate that lignin is the most sensitive component of heat-treated birch to the weathering degradation process. Elimination of the amorphous and highly crystallised cellulose is observed for both heat-treated and untreated wood during weathering. It is also observed that heat treatment increases the lignin and crystallised cellulose contents, which to some extent protects heat-treated birch against degradation due to weathering.

Keywords: Heat-treated wood; artificial weathering; FTIR; wood chemical component; SEM; structural change

1. Introduction

The weathering of untreated wood causes roughening and cracking of wood surface and damages its microstructure. Untreated wood exposed to outdoor weathering undergoes checking and surface erosion principally due to the effects of solar radiation and stresses imposed by cyclic wetting, temperature changes, environmental pollutants, and certain micro-organisms [1]. A number of researchers have examined the effect of weathering on the physical structure of wood [1-8]. Microscopic studies showed characteristic ridges on the S3 wall layer, wall checking, ray and pit degradation, and middle lamella breakdown. Several publications describe similar observations related to microscopic changes found on untreated wood surfaces which were artificially

weathered by exposure to UV irradiation [9-11]. Changes observed on the wood surfaces due to artificial weathering were very similar to those caused by natural outdoor weathering [12]. The effect of weathering on the chemical structure of wood was also studied by means of FTIR spectroscopy [13]. These studies generally have been carried out for untreated wood.

High-temperature heat-treated wood is a relatively new product which is heated to high temperatures in the range of 180 and 260°C, depending on the species used and the desired material properties [14]. A few researchers have studied the micro-structural properties of heat-treated wood by means of SEM. Boonstra et al. [15, 16] found that heat treatment had an effect on the anatomical structure of wood, and the extent of this effect depended on the wood species and the treatment method and conditions used. Softwood species with narrow annual rings which had an abrupt transition from earlywood to latewood were sensitive to tangential cracks in the latewood section. Radial cracks occurred mainly in impermeable wood species such as Norwegian spruce, caused by large stresses in the wood structure during treatment. Sapwood of treated pine species revealed some damage to parenchyma cells in the rays and epithelial cells around resin canals while this phenomenon was not noticed in the heartwood section [16]. However, it was found that the anatomical structure of wood was only slightly affected during heat treatment [17]. Vessels, fibers, parenchyma, and rays were still intact after the heat treatment. The main effect of heat treatment was the presence of significant quantities of extractives deposited in the vessels, which normally disappear after heat treatment. Heat treatment changes both chemical and physical properties of wood. The decrease of amorphous polysaccharide content (hemicelluloses), condensation and demethoxylation of lignin, and the removal of certain extractives occurring due to heat treatment at high temperatures were reported by different researchers [18-20]. As a result, heat-treated wood possesses new physical properties such as reduced hygroscopy, improved dimensional stability, better resistance to degradation by insects and micro-organisms, and most importantly, attractive darker color. The new versatile properties make heat-treated wood popular for outdoor applications.

As explained above, various studies were carried out on the structural analysis of untreated and heat-treated wood, and weathering of untreated wood. Most of the previous studies on structural changes due to weathering of heat-treated wood were limited to the study of physical structure investigated using SEM. To the authors' knowledge, although there are several previous studies on the effect of weathering on the surface properties (such as changes in wettability) of heat-treated woods [21-23], a detailed and comprehensive study of physical and chemical structural changes of heat-treated wood including fluorescence microscopy, SEM, and FTIR are not available in the literature; and, structural changes of heat-treated wood due to weathering are not completely

understood. Furthermore, there is no published study available on the structural analysis of wood that is heat-treated under different heat treatment conditions and then subjected to weathering. The present study aims to fill this void.

The objectives of this study are to investigate the detailed physical micro-structural variations and chemical structural changes the different components of heat-treated wood undergo due to accelerated artificial weathering and to identify the relation between the physical structural changes and the chemical degradation of wood components. The effect of different heat treatment conditions (such as temperature) on the artificial weathering degradation process was also studied. The type of wood studied is the hardwood birch (*Betula papyrifera*). The birch wood is popular in the North American market, especially in Quebec, and the heat-treated wood has diverse outside uses.

2. Material and methods

2.1. Material

Birch (*Betula papyrifera*), a hardwood that is commonly used for outdoor applications in North America, was studied. After heat-treated birch boards were subjected to artificial weathering. Untreated wood boards, kiln dried to a final moisture content of about 12%, were also exposed to artificial weathering along with heat-treated specimens for comparison purposes. Specimens were arbitrarily selected for a complete statistical randomization. They were stored in a room at 20°C and 40% relative humidity (RH) until they were exposed to artificial weathering and then characterized using the tests described below.

Specimens of 70 × 65 mm cross-section on longitudinal surfaces and 20 mm in length were cut from sapwood of heat-treated and untreated wood, and then planed to have smooth surfaces. The prepared specimens were used in artificial weathering tests. The color evaluation was carried out on both longitudinal tangential surface (LT) and longitudinal radial surface (LR) of the wood samples.

2.2. Artificial weathering tests

Artificial weathering tests were conducted at the Laval University in collaboration with FPInnovation. The samples were exposed to UV light in a commercial chamber, Atlas Material Testing Technology LLC (USA) Ci65/Ci65A Xenon Weather-Ometer. A controlled irradiance water-cooled xenon arc with a CIRA inner filter and a Soda outer filter was used as the source of radiation to simulate sunlight. Tests were performed according to Cycle 1 of Standard ASTM G155: 102 min Xenon light, 18 min light and water spray (air temperature is not controlled) without dark cycle to simulate rain in natural weathering. The black panel temperature was set to

63±3°C and the irradiance level was 0.35W/m² at 340 nm. Heat-treated samples and untreated control samples were exposed to UV light. The irradiation was interrupted after 72, 168, 336, 672, 1008, and 1512 h of exposure, and two samples for each set of experimental conditions were taken out for evaluation of changes in chemical and physical structure.

2.3. Fluorescence microscopy analysis

Structural properties of untreated and heat-treated wood before and after weathering were investigated. Transverse sections cut through wood at a thickness of 7-20 µm were examined and photographed with the Nikon eclipse E600 microscope. Some sections were also stained with 0.05% aqueous toluidine blue prior to examination with the photomicroscope. Light microscopy was also undertaken on sections that had been stained with 1% aqueous osmium tetroxide (OsO₄) for 10–30 min at room temperature. Sections for scanning electron microscopy were cut from the same blocks from which the sections for light microscopy were taken.

2.4. Scanning electron microscopy (SEM) analysis

Small wood blocks measuring 20 ×20 mm on the weathered tangential face were cut from heat-treated and untreated boards after artificial weathering for different times (0, 336, 672 and 1512 h). For subsurface cell degradation analysis, same blocks measuring 20 ×10 mm on the transverse face and radial face were used. The specimens were immersed in water for 30 minutes. Then, one of the end-grain surfaces and one radial surface were carefully cut with a razor blade mounted onto a microtome. A new razor blade was used for each final cut. Another method of preparation for SEM analysis is to split wood samples. However, these surfaces were rough, and they usually did not allow observation of the cell lumen. The specimens were washed in distilled water to remove the bleaching agent and then air-dried at room temperature for more than two nights, and desiccated with phosphorus pentoxide for 10 days. Finally, all blocks were sputter-coated with a palladium/gold layer (20 nm) and then mounted onto standard aluminum stubs using electrically conducting paste. The samples were scanned using a Jeol scanning electron microscope (JSM 6480LV) with a magnification up to 300000× at 10kV of accelerating voltage. The distance between sample and electron microscope head was 20-25 mm with a spot size of 35. The specimen temperature was approximately 20°C and the column vacuum was 6.66×10⁴ Pa. Electron micrographs of the UV irradiated longitudinal tangential surfaces for different exposure times were taken. SEM micrographs of longitudinal radial surfaces were also taken to observe the cell damage from the radial direction.

2.5. FTIR spectroscopy analysis

The effect of sunlight irradiation on chemical compositions of both cellulose and lignin and cellulose crystallinity on wood surface were studied using Fourier transform infrared (FTIR) spectroscopy. The air-dried specimens (10×20×20 mm) were studied using Jasco FT/IR 4200 equipped with a diamond micro-ATR crystal. IR spectra were recorded in the wave number range of 550–4000 cm^{-1} at 4 cm^{-1} resolution for 20 scans prior to the Fourier transformation. The incident angle of the micro-ATR crystal was 47° corresponding to the sampling depth of the infrared radiation of 0.2–5 μm , depending on the wave number. This ensured that the recorded IR spectra of wood surfaces were sufficiently surface sensitive. Thus, changes in IR spectral features were solely caused by changes in surface chemistry, and there was no change of underlying bulk chemistry of the wood specimen. The aperture diameter was 7.1mm. All spectra were analyzed using Jasco spectra manager software. The FTIR spectra were corrected by the FTIR software package which includes an ATR correction algorithm. All intensity ratios were normalized by using the peak intensity at 2900 cm^{-1} which is C-H stretching in methyl and methylene groups.

2.6. Heat treatment

Birch woods were heat-treated in a prototype furnace of the University of Quebec at Chicoutimi (UQAC), Quebec, Canada. The natural gas was used to heat the furnace. Thus, the wood was in contact with hot, humid and inert combustion gases (nitrogen, water vapor and carbon dioxide) during the treatment. The presence of humidity is important, which acts as a screen gas and protects the wood from oxidation [24]. Water was evaporated and injected into the gas to simulate the presence of humidity. Table 1 shows the conditions of the heat treatment. During each tests, four wood boards of approximately 6500 × 200 × 30 mm were heated gradually until a predetermined maximum temperature (195-215°C). When this temperature was reached, it was maintained for a period of 1h (which is called holding time) in order to homogenize the temperature distribution within the wood as much as possible. The woods were then cooled down with direct water spray.

3. Results and discussion

3.1. Visual observation of surface appearance

Figures 1a, 1b, 1c, and 1d compare the color changes and the physical changes taking place during artificial weathering on the tangential surfaces of birch samples, untreated and heat-treated at different temperatures. It

can be observed that the color of all untreated samples and those of heat-treated at three different temperatures become lighter and whiter with increasing weathering time, but at different rates. However, it is difficult to analyze the structural changes of the samples based only on their visual appearance. A detailed analysis of structural changes with the fluorescence microscopy and the scanning electron microscopy were carried out and are presented below.

3.2. Structural analysis with fluorescent microscopy

Fig. 2 shows the fluorescence microscopy images of untreated birch as well as birch samples heat-treated at two different temperatures (195°C and 215°C) for different weathering times (0h, 72h, 672h, 1512h) and compares them with those of non-aged wood. After 72 h of exposure, the damage of two cell layers is visible for untreated birch (Fig. 2 (b)) while damage of one cell layer is visible for those heat-treated at 195°C (Fig. 2 (f)). However, for the birch wood which was heat-treated at a temperature of 215°C, no damage of wood cells on test surface is visible after 72 h weathering (Fig. 2 (j)). This indicates that heat treatment increases the resistance to weathering of the structure of birch wood. The degradation of cells increases with increasing exposure time for both heat-treated and untreated birch. Delamination and thinning of cells appear after weathering of 672 h for all samples in this study (Fig. 2 (c, g, k)). From the comparison of fluorescence microscopy images of the heat-treated and untreated birch samples exposed to accelerated aging for different times, it can be observed that the degradation increases with increasing exposure time for all samples. The degree of damage to wood heat-treated at 215°C is less compared to that of untreated wood and wood heat-treated at 195°C at the same weathering time. This indicates that increase in heat treatment temperature increases the structural resistance of birch wood against weathering.

3.3. Structural analysis by means of SEM

a) Transverse surfaces

Fig. 3 shows the surface micrographs on transverse surfaces of untreated and heat-treated woods before and after artificial weathering for 1512 h. Comparing Fig. 3 (a), (c) and (e), it can be seen that the slight thinning of cell wall on middle lamella takes place on birch transverse surface after heat treatment at both 195°C and 215°C. Nevertheless, it seems that there is no cracking. Heat-treated birch wood looks more brittle than its untreated counterpart. However, structural changes due to heat treatment are not distinct, and it is likely that plasticization of cell wall material occurs only to a limited degree during heat treatment. This is in agreement

with the results of Kollmann and Sachs who found comparable features in spruce after heat treatment between 190°C and 240°C [16] and the results of previous studies by Huang et al. [22, 25]. Compared to sample heat-treated at 195°C, the sample heat-treated at 215°C displays more significant structural changes due to heat treatment as seen in Fig. 3 (e), showing more thinning of the cell wall width. Fig. 3 (b), (d), and (f) show the micro-structural changes of cell occurring after artificial weathering for 1512 h on the transverse surfaces of untreated birch, and birch heat-treated at 195°C and 215°C, respectively. The significant thinning of cell wall width for all specimens take place compared to samples before weathering; however, their magnitude which is different for different samples is difficult to differentiate after the weathering of 1512 h. The development of cracks on the cell wall of the specimen heat-treated at 215°C is observed (see arrow in Fig. 3 (f)), however it is difficult to identify the structure of cell wall for the untreated sample after the weathering of 1512 h. This indicates that the effect of weathering on the cell wall of untreated birch surface is more than on that of heat-treated samples.

b) Longitudinal surfaces

Additional information on micro-structural changes can be seen from the SEM micrographs on longitudinal surfaces of the specimens. Fig. 4 shows the SEM micrographs on longitudinal tangential surfaces of untreated and heat-treated specimens before and after weathering for different times. The lumen of fibers of untreated birch is attached to some warty membrane inside the S3 layer (see arrows in Fig. 4 (a)), which disappears in the lumen of heat-treated wood fibers in cell walls (see Fig. 4 (b) and (c)); and this is similar to the results of jack pine reported in a previous study [25]. As shown in Fig. 4 (a) and (b), there is no noticeable difference on the cell wall and pits of untreated and heat-treated specimens at 195°C; however, micro-cracks originated from pits are observed on the cell wall of samples heat-treated at 215°C (see arrow in Fig. 4 (c)). These micro-checks appear to be a result of the stress caused by differential shrinkage due to heat treatment. The SEM analysis indicates that the anatomical structure of wood is hardly affected when heat-treated at low temperature and only slightly affected when temperature increases to 215°C. This result is in agreement with the previous research [26] which reported that the main differences were the presence of important quantities of extractives deposited in the resin channels that disappeared after heat treatment. The micrographs of tangential surfaces also show the degradation during artificial weathering (see Fig. 4 (c-n)). After artificial weathering for 72 h, longitudinal micro-cracks aligned with the fibril orientation and diagonal to the fiber axis of the fiber cells were observed for all samples (see Fig. 4 (d, e, f)). Micro-cracks develop and enlarge principally as a result of the degradation of lignin, which is the binder of cellulose microfibrils in the various cell wall layers, as well as the contraction in

cell walls caused by water spray during artificial weathering. Fig. 4 (g, h, i) show the SEM micrographs of samples exposed for 672 h. The comparison of these surfaces with those weathered for 72 h reveals the difference in damage due to different exposure times. The existence of ray cells on untreated sample surfaces weathered for 72 h can be observed. However, all ray cells disappear from the surfaces after weathering for 672 h; consequently, only cavities remain and abundant uniseriates and longitudinal micro-checks occur (see Fig. 4 (g, h, i)). In contrast, no transversal checks of cell wall are observed. After weathering for 1512 h, large longitudinal micro-cracks originating from the degradation of ray cells are seen, and transverse micro-cracks caused by the breakage of microfibril become evident (see arrows in Fig. 4 (j, k, n)). A separation between two adjacent cells occurs and fiber cells loosen, collapse, and detach from the substrate of heat-treated wood (enlarged image in Fig. 4 (n)).

Differences in degradation behavior are observed for untreated and heat-treated birch wood are shown in Fig.4 (g, h i). The cracks of the sample heat-treated at 215°C are less than those of untreated and heat-treated wood at 195°C. This indicates that the higher heat-treatment temperature has a more protective effect on structural changes during weathering, which is in agreement with the results of the florescence microscopy analysis. The differences observed in structural changes might be related to the chemical changes taking place during heat treatment. Heat-treated wood contains more lignin and less cellulose compared to those of untreated wood [23]. However, their magnitude which is different for different heat treatment conditions is difficult to differentiate after the weathering of 1512 h (see Fig. 4 (j, k, n)).

Fig. 5 shows the SEM micrographs for the evaluation of the damage on bordered pits between fibers and vessels of birch sample heat-treated at 215°C. Heat treatment does not cause damage to the bordered pits (see Fig. 5(a)). Pit cracks formed on the wood surface after weathering for 72 h are small and do not cause the failure of pits (Fig.5 (b)). Coalesce originating from pits increase on the surface after weathering for 672 h; later on, ruptured cracks form (Fig.5 (c)). The degradation of pits between vessel and fiber cells of heat-treated birch after weathering for 1512 h enlarges and the pit borders thin. Although, it becomes thinner, the pit tissue still can be clearly observed (Fig. 5 (d)).

3.4. Structural analysis with FTIR spectroscopy

In this study, the results of the infrared study of artificial weathering on heat-treated samples are presented and compared with those of untreated samples in order to investigate the details of structural changes in chemical

components of heat-treated birch. The most representative FTIR bands studied within the spectral range of 4000-550 cm^{-1} were summarized in previous studies [22, 25].

3.4.1. Spectral characterization of untreated and heat-treated birch

The differences in spectra between heat-treated and untreated woods have to be taken into consideration to better understand the structural changes taking place during heat treatment. Fig. 6 shows the FTIR spectra between the spectral regions of 1800-1400 cm^{-1} and 1400-1100 cm^{-1} of untreated birch and samples heat-treated at three different temperatures before artificial weathering. Table 2 illustrates the variation in the average absorbance values of the different selected functional groups observed during heat treatment and artificial weathering. The quantitative values that appear in Table 2 are only used qualitatively in the discussion of the results.

The four spectra shown in Figure 6 present different infrared spectra for untreated and heat-treated birch before weathering. The infrared spectra of samples heat-treated at different temperatures in the studied region had some similar features. Upon analysis of the spectra, it can be seen that the relative intensity of band at 1740 cm^{-1} , which is a characteristic band for non-conjugated carbonyl group stretching in xylan in hemicelluloses [13], decreases slightly after heat treatment (see Fig. 6 and Table 2).

It can be observed that the bands at 1600 cm^{-1} , 1510 cm^{-1} , and 1457 cm^{-1} , which are assigned to lignin [13, 27], increase slightly after heat treatment at all temperatures. This indicates that the degradation of hemicelluloses subsequently causes an increase in the lignin component of wood. The peak of 1510 cm^{-1} indicates the splitting of the aliphatic side chains in lignin and cross linking formation by condensation reactions of lignin. The observed increase of these peaks are in agreement with the results of previous studies [22, 28] which showed that the chemical changes occurring result in a decrease in water absorption and, consequently, increase in dimensional stability.

Another peak which has to be taken into consideration is the one at 1230 cm^{-1} which is a characteristic of syringyl nuclei [13]. This peak increases after heat treatment at 195°C and 200°C and then decreases at 215°C. This indicates that the degradation of lignin also occurs during heat treatment and the treatment temperature affects the quantity of wood components present in wood after the treatment.

The peaks of 1420 cm^{-1} , 1335 cm^{-1} , and 1318 cm^{-1} (see Fig.6 and Table 2) are assigned to the cellulose component, and the 1335-1318 cm^{-1} doublet is related to the crystallised I and amorphous cellulose contents [13]. Increases in these two peaks can be observed after heat treatment at all three treatment temperatures

studied (Table 2). An increase in the ratio $1335/1318\text{ cm}^{-1}$ indicates a decrease in crystallinity. Based on these results, it can be said that heat treatment increases the crystallised cellulose content (see Fig. 8 (c)).

The increase in C–O peak at 1103 cm^{-1} after heat treatment might indicate the formation of new alcohols and esters, which can reduce the number of the free hydroxyl groups and, consequently, increase the hydrophobic character of wood [13, 22, 28].

3.4.2. Structural and chemical changes in wood components due to artificial weathering

Fig. 7 (a-c) shows the FTIR spectra in the spectral regions of birch heat-treated at 195°C , 205°C , and 215°C after artificial weathering for different periods, respectively. An analysis of the changes in FTIR spectra of the woods heat treated at different temperatures and subjected to artificial weathering (Table 2 and Figs. 7 (a-c)) allows the following conclusions to be deduced. It is apparent from the overall IR spectrum of the three heat-treated samples that a number of spectral features appear to be sensitive to artificial weathering. Although the change in the IR spectrum of birch heat-treated at different temperatures due to artificial weathering have some similar features, each experimental set has a different spectrum pattern (see Fig. 7 (a-c)). All the changes in FTIR spectra for the three heat-treated birch wood surfaces, brought about by the weathering process, are essentially complete sometime between 672 and 1512 h of weathering. After the specimens have been subjected to 1512 h of artificial weathering with simulated sunlight and water spray, the FTIR spectra of all three heat-treated woods are found to be very similar.

As shown in Table 2, the absorbance at 1740 cm^{-1} , assigned to carbonyl groups [29] and C=O stretching vibration of acetyl or carboxylic acid of hemicelluloses [13, 30], decreases after weathering for all three heat-treated samples, thus indicating a decrease in hemicelluloses. The absorbance at 1370 cm^{-1} is mainly due to carbohydrates (cellulose and hemicelluloses). It has no significant contribution from lignin and is not affected significantly by weathering (see Fig. 7). The proportion of carbonyl groups during artificial weathering was calculated by taking the ratio of the intensity of the carbonyl band at 1740 cm^{-1} over that of the carbohydrates peaks at 1370 cm^{-1} . The ratio of the intensity of C=O band at 1740 cm^{-1} to 1370 cm^{-1} band represents the relative changes of carbonyl groups due to exposure to weathering. The relative changes in the ratio of carbonyl peak at 1740 cm^{-1} (I_{carbonyl}) over carbohydrates peaks at 1370 cm^{-1} ($I_{\text{carbohydrates}}$) for heat-treated and untreated birch as a function of weathering time are presented in Fig. 8 (a). The ratio I_{1740}/I_{1370} of three samples decreases during the weathering process. Thus, the above results indicate that the unconjugated carbonyl group at 1740 cm^{-1} is decreased. This is in agreement with the finding reported by Masanori and Tokato [31]. They found that the

unconjugated carbonyl group at 1740 cm^{-1} decreased with more than 50 h of exposure for untreated tropical wood. Huang et al. [25] also observed that the band at 1740 cm^{-1} of heat-treated jack pine decreased due to artificial sunlight exposure from 72 h to 1500 h. However, Pandey reported the opposite result for untreated chir pine and rubber wood [32]. These different findings might be due to the differences in wood species and modifications during heat treatment.

As Fig.7 shows, the new bands at 1650 cm^{-1} can be detected in the present study for three heat-treated wood surfaces after weathering for 72 h and 672 h, and then the intensity of this band reduces after weathering for 1512 h. The increase in this band might be due to the formation of quinines and quinone methides (responsible for the yellowing of wood surface) resulted from the exposure to UV irradiation while the decrease is related to the leaching of these products by water spray after a long exposure to artificial weathering. Erin et al. [29] reported similar results and stated that the new band was generated and this band changes depending on artificial weathering conditions.

As stated in a previous study [22], all the bands at 1600 cm^{-1} , 1510 cm^{-1} , 1457 cm^{-1} , 1235 cm^{-1} , and 1103 cm^{-1} represent lignin characteristics. As shown in Fig.7 (a-c) and Table 2, all these characteristic bands of lignin decrease significantly as a result of the weathering process for all heat-treated birch surfaces. This indicates that lignin is the component of heat-treated wood which is most degraded during weathering. This is in accordance with the results of the chemical component analysis of heat-treated wood after weathering reported in another previous study [23]. The peaks at 1600 cm^{-1} and 1510 cm^{-1} are mainly the characteristic absorption of C=C in an aromatic ring that originated from lignin in wood [13, 27]. It can be observed from Fig. 7 that both of these peaks disappear after the weathering of 72 h for the samples heat-treated at all three temperatures in this study. This is in agreement with the results of the previous studies on untreated wood by Pandey [54] and heat-treated jack pine wood by Huang et al. [25]. The peak at 1457 cm^{-1} is assigned to C-H asymmetric bending in CH_3 of lignin and the peak at 1235 cm^{-1} is contributed to syringyl nuclei [13]. The decrease in intensity of these two peaks occur after weathering for 72 h, and then they disappear after 1512 h. Slight changes take place for the peak at 1103 cm^{-1} , which is related to C-H in guaiacyl and syringyl of lignin [33].

From the five bands mentioned above, the evolution of the lignin loss is best explained by the band at 1510 cm^{-1} of the heat-treated birch wood samples. The lignin loss for heat-treated and untreated wood specimens for birch after artificial weathering at different times were measured as suggested in the literature [22] and plotted in Fig.8 (b). All heat-treated wood surfaces show higher lignin content than those of untreated wood surfaces

before weathering. The lignin content increases as the heat treatment temperature increases. During the first exposure period of artificial weathering for 72 h, lignin in all specimens becomes degraded although a large difference can be seen in the evolution of the degradation process. The decrease observed for this band is significantly larger in the case of heat-treated wood than that of untreated sample after 72 h of weathering. The significant decrease in the intensity of lignin peak intensity shows rapid lignin degradation in the beginning of weathering for heat-treated birch. After this time, a slight decrease can be observed for both heat-treated and untreated woods up to 1512 h of weathering. Lignin of heat-treated birch samples is degraded at a faster rate than that of untreated samples, which is in agreement with the results of jack pine wood during exposure to artificial sunlight irradiation [25]. The difference in lignin content between untreated wood and woods heat-treated at different temperatures reduces significantly, and they become relatively close after weathering for 1512 h. This indicates that long periods of weathering decreases the differences in chemical characteristics of heat-treated and untreated birch surfaces, which supports the findings on micro-structural changes discussed above.

The peak at 1420 cm^{-1} , which is characteristic of CH_2 aromatic skeletal vibrations of lignin and C-H deformation in plane in crystallised cellulose I and amorphous cellulose mixture [13, 34], shows a very similar evolution for the three heat-treated birch samples (see Table 2). The behaviour of the band at 1420 cm^{-1} (see Fig.7), which is a characteristic of crystallised cellulose I according to Colom and his co-workers [13], indicates that the amorphous area of the cellulosic component of three heat-treated woods is affected by the degradation process. Similar findings for untreated box and aspen wood were also reported [13].

The band at 1335 cm^{-1} and the band at 1318 cm^{-1} are assigned to the phenol group of wood cellulosic component and high crystallised cellulose I, respectively [13]. Slight increases in intensity of both of these two peaks can be observed after 72 h of weathering for all heat-treated specimens, but not for untreated wood (see Table 2). This can be interpreted as an increase in the relative cellulose content for both amorphous and high crystallised cellulose in the heat-treated birch samples as a result of significant lignin component degradation at beginning of weathering. Afterwards, the intensities at these peaks enhance, which indicates that amorphous and high crystallised cellulose of heat-treated birch are also degraded at longer exposure times. As stated above, the spectroscopic evolution of the ratio $1335/1318\text{ cm}^{-1}$ contributes to the degradation process of amorphous cellulose and high crystallised cellulose I during weathering. The evolution of the ratio $1335/1318\text{ cm}^{-1}$ as a function of weathering time is plotted in Fig. 8 (c) and is used to monitor the degradation process [13]. A

decrease in the ratio $1335/1318\text{ cm}^{-1}$ indicates an increase in crystallinity. It can be observed that in untreated and all three heat-treated woods the degradation process is more intense in the amorphous cellulose component than in the crystallised cellulose I component at the initial time of weathering for 72 h. The $1335/1318\text{ cm}^{-1}$ ratios change slightly at longer exposure times. This means that the degradation extents of amorphous cellulose and high crystallised cellulose I become close when samples are weathered for a long period. A detailed analysis of this ratio shows that changes in this ratio for heat-treated birch are lower than that of untreated wood during the initial stage of weathering. This indicates that the cellulose is more stable in heat-treated wood than in untreated wood. The higher stability of cellulose might be linked to the protection of higher lignin content on heat-treated wood surface. The improvement of lignin content after heat treatment might explain the improvement in color stability of heat-treated woods during the earlier times of weathering [23].

The peak at 1200 cm^{-1} , originating from the O-H deformation in cellulose [33, 34], shows a similar behaviour in each case (Fig. 7 (a-c)). This band undergoes a progressive increase and stabilises after 72 h of weathering. This behaviour might be interpreted as the reflection of a more stable structure for the cellulosic component than for the lignin component during weathering. The increase in absorption at this peak is mainly due to the increase in relative cellulose content in the heat-treated samples after weathering. In a previous study [23], it was shown that the heat-treated wood surface after weathering was rich in cellulose but poor in lignin content, which confirms the behavior of this band. Moreover, the intensities of 1158 cm^{-1} band, assigned to C-O-C group in carbohydrate [32, 34], increase upon prolonged exposure indicating that lignin is the component of heat-treated wood which is most degraded during weathering.

The total crystallinity index (H_{1370}/H_{2900}) and the lateral order index (H_{1429}/H_{898}) is determined from the absorption ratios for both heat-treated and untreated specimens [35] and plotted in Fig. 9 (a) and (b), respectively. The values of total crystallinity index refer to the sum of cellulose I and cellulose II values and the lateral order index refers to cellulose I [13]. A decrease in the crystallinity of all specimens can be observed from Fig. 9. The results show that changes occur to different extents depending on different heat treatment conditions. This demonstrates that crystalline cellulose, including both cellulose I and cellulose II, degrades although during the initial stage of weathering for 72 h (indicated by the spectra of the band at $1335-1318\text{ cm}^{-1}$) the degradation of crystalline cellulose is less severe than that of amorphous cellulose component. The crystallinities from both indexes of all heat-treated specimens are higher than those of untreated woods for all weathering times. This means that the heat treatment degrades more the amorphous cellulose components

compared to the crystallised cellulose. The similar observation is reported by Mehmet and his colleagues [36]. They stated that the crystallinity of both Scots pine and Uludag fir increased during heat treatment. Also, the loss of crystallinity of heat-treated jack pine wood during simulated sunlight exposure was also observed in a previous study of Huang et al. [25]. This raises the amorphous portion of cellulose and, consequently, increases the hydrophilic nature of weathered wood surface.

3.4.3. Weathering mechanisms of heat-treated birch

In this study, the results show that the lignin of heat-treated birch woods is degraded due to exposure to artificial weathering. Based on the experimental and characterization results discussed above, the following photo-degradation mechanism for heat-treated birch wood is proposed. Lignin is an amorphous three-dimensional polyphenolic material in which the aromatic ring units are connected with ether and C–C bonds in a helical structure [37]. Lignin is degraded by the cleavage of C=C bonds of the aromatic ring as confirmed by the elimination or disappearance of peaks at 1600 and 1510 cm^{-1} in the FTIR spectra. The UV radiation energy during weathering is absorbed by the α -carbonyl group of lignin, which induces the α -carbonyl group to transfer into an excited state [38]. Consequently, the linkages between the aromatic ring units in lignin are initiated to cleave. After several electron migration steps, quinines and quinone methides are formed. This is confirmed by the growth of peaks at 1650 cm^{-1} (see Fig.7). These products might be accompanied by a color change [29]. As the weathering continues, spray water during the artificial weathering washes out the chromaphoric by-products formed by the degradation of lignin which are present on the heat-treated wood surface (see Fig. 10 (a)). This degradation results in heat-treated birch surface to become richer in cellulose and poorer in lignin after weathering. Then, the exposed surface goes through further degradation. Both amorphous cellulose component and crystallized cellulose region are attacked; the later component is damaged and transformed to amorphous state. Consequently, micro-cracks and macro-cracks form after weathering (see Fig. 10 (b)). This is explained by the evaluation of crystallinity changes during weathering (see Fig.9). Furthermore, the cleavages of units in cellulose fibrils take place, which produces many crystalline defects throughout the whole fibrils (see Fig.10 (c)). It reveals that the fibrils are broken to isolated arrays of short fragments.

4. Conclusions

The results of the fluorescent microscopy analysis show that the degradation due to weathering increases with increasing exposure time for untreated and heat-treated birch woods. However, heat treatment increases

structural resistance of birch wood against weathering and this becomes more and more prevalent with increasing heat treatment temperature. Therefore, the effect of weathering on the cell wall of untreated birch surface is more significant than on that of heat-treated samples. The degradation of hemicelluloses can consequently cause an increase in lignin component of birch wood. Lignin content increases slightly with heat treatment. This increase becomes more important as the treatment temperature increases. It is also found that the heat treatment increases the crystallised cellulose content. The increase in lignin and crystallised cellulose contents brought about by heat treatment protects heat-treated birch against degradation taking place during weathering.

Acknowledgements

The authors thank Fonds québécois de la recherche sur la nature et les technologies (FQRNT), Développement Économique Canada (DEC), Ministère du Développement Économique, de l'Innovation et de l'Exportation (MDEIE), Conférence Régionale des Élus du Saguenay-Lac-St-Jean (CRÉ), Université du Québec à Chicoutimi (UQAC), Fondation de l'Université du Québec à Chicoutimi (FUQAC), FPIInnovation, Alberta Innovates, and industrial partners (PCI Ind., Kisis Technology, and Industries ISA), for their technical and financial contributions. The authors also thank the Centre universitaire de recherche sur l'aluminium (CURAL) at UQAC for valuable assistance and technical support during SEM analysis.

References

- [1] R.S. Williams, W.C. Feist, Application of ESCA to evaluate wood and cellulose surfaces modified by aqueous chromium trioxide treatment, *Colloids and Surfaces*, 9 (1984) 253-271.
- [2] D.N.S. Hon, Cellulose: a random walk along its historical path, *Cellulose*, 1 (1994) 1-25.
- [3] E.R. Miller, H. Derbyshire, PHOTODEGRADATION OF WOOD DURING SOLAR IRRADIATION, in, NBS, Gaithersburg, MD, USA, 1981, pp. 279-287.
- [4] D.N.S. Hon, ESCA STUDY OF OXIDIZED WOOD SURFACES, *Journal of Applied Polymer Science*, 29 (1984) 2777-2784.
- [5] D.N.S. Hon, S.-T. Chang, SURFACE DEGRADATION OF WOOD BY ULTRAVIOLET LIGHT, *Journal of polymer science. Part A-1, Polymer chemistry*, 22 (1984) 2227-2241.
- [6] P.D. Evans, A.J. Michell, K.J. Schmalzl, Studies of the degradation and protection of wood surfaces, *Wood Science and Technology*, 26 (1992) 151-163.

- [7] P.D. Evans, P.D. Thay, K.J. Schmalzl, Degradation of wood surfaces during natural weathering. Effects on lignin and cellulose and on the adhesion of acrylic latex primers, *Wood Science and Technology*, 30 (1996) 411-422.
- [8] K. Borgin, N. Parameswaran, W. Liese, The effect of aging on the ultrastructure of wood, *Wood Science and Technology*, 9 (1975) 87-98.
- [9] V.P. Miniutti, Microscale changes in cell structure at softwood surfaces during weathering, *Forest Prod. J.*, 14 (1964) 571-576.
- [10] L.P. Futo, Der photochemische Abbau des Holzes als Präparations- und Analysenmethode, *Holz Roh-Werkstoff*, 32 (1974) 303-311.
- [11] M.-L. Kuo, Hu, N., Ultrastructural changes of photodegradation of wood surfaces exposed to UV, *Holzforschung*, (1991) 45, pp. 347-353.
- [12] P.D. Evans, Structural changes in *Pinus radiata* during weathering, *J. Inst. Wood Sci.*, 11 (1989) 172-181.
- [13] X. Colom, F. Carrillo, F. Nogués, P. Garriga, Structural analysis of photodegraded wood by means of FTIR spectroscopy, *Polymer Degradation and Stability*, 80 (2003) 543-549.
- [14] D. Kocafe, J.L. Shi, D.Q. Yang, M. Bouazara, Mechanical properties, dimensional stability, and mold resistance of heat-treated jack pine and aspen, *Forest Products Journal*, 58 (2008) 88-93.
- [15] M.J. Boonstra, J.F. Rijdsdijk, C. Sander, E. Kegel, B. Tjeerdsma, H. Militz, J. Van Acker, M. Stevens, Microstructural and physical aspects of heat treated wood. Part 2. Hardwoods, *Maderas: Ciencia y Tecnologia*, 8 (2006) 209-217.
- [16] M.J. Boonstra, J.F. Rijdsdijk, C. Sander, E. Kegel, B. Tjeerdsma, H. Militz, J. Van Acker, M. Stevens, Microstructural and physical aspects of heat treated wood. Part 1. Softwoods, *Maderas: Ciencia y Tecnologia*, 8 (2006) 193-208.
- [17] b. Francis Mburu a, Stephane Dumarcay a, Françoise Huber a, Mathieu Petrissans a., Philippe Gerardin a, Evaluation of thermally modified *Grevillea robusta* heartwood as an alternative to shortage of wood resource in Kenya: Characterisation of physicochemical properties and improvement of bio-resistance, *Bioresource Technology*, (2007).
- [18] M. Nuopponen, H. Wikberg, T. Vuorinen, S.L. Maunu, S. Jämsä, P. Viitaniemi, Heat-treated softwood exposed to weathering, *Journal of Applied Polymer Science*, 91 (2004) 2128-2134.
- [19] H. Sivonen, S.L. Maunu, F. Sundholm, S. Jämsä, P. Viitaniemi, Magnetic resonance studies of thermally modified wood, *Holzforschung*, 56 (2002) 648-654.

- [20] R. Kotilainen, R. Alén, V. Arpiainen, Changes in the chemical composition of Norway spruce (*Picea abies*) at 160-260°C under nitrogen and air atmospheres, *Paperi ja Puu/Paper and Timber*, 81 (1999) 384-388.
- [21] X. Huang, D. Kocaefe, Y. Boluk, Y. Kocaefe, A. Pichette, Effect of surface preparation on the wettability of heat-treated jack pine wood surface by different liquids, *European Journal of Wood and Wood Products*, (2012) 1-7.
- [22] X. Huang, D. Kocaefe, Y. Kocaefe, Y. Boluk, A. Pichette, Changes in wettability of heat-treated wood due to artificial weathering, *Wood Science and Technology*, (2012) 1-23.
- [23] X. Huang, D. Kocaefe, Y. Kocaefe, Y. Boluk, A. Pichette, A spectrophotometric and chemical study on color modification of heat-treated wood during artificial weathering, *Applied Surface Science*, 258 (2012) 5360-5369.
- [24] S. Poncsak, D. Kocaefe, R. Younsi, Y. Kocaefe, L. Gastonguay, Thermal treatment of electrical poles, *Wood Science and Technology*, 43 (2009) 471-486.
- [25] X. Huang, D. Kocaefe, Y. Kocaefe, Y. Boluk, A. Pichette, Study of the degradation behavior of heat-treated jack pine (*Pinus banksiana*) under artificial sunlight irradiation, *Polymer Degradation and Stability*, (2012).
- [26] F. Mburu, S. Dumarçay, F. Huber, M. Petrisans, P. Gérardin, Evaluation of thermally modified *Grevillea robusta* heartwood as an alternative to shortage of wood resource in Kenya: Characterisation of physicochemical properties and improvement of bio-resistance, *Bioresource Technology*, 98 (2007) 3478-3486.
- [27] A. Temiz, N. Terziev, M. Eikenes, J. Hafren, Effect of accelerated weathering on surface chemistry of modified wood, *Applied Surface Science*, 253 (2007) 5355-5362.
- [28] D. Kocaefe, S. Poncsak, Y. Boluk, Effect of thermal treatment on the chemical composition and mechanical properties of birch and aspen, *BioResources*, 3 (2008) 517-537.
- [29] E.L.P. Anderson, Zenon1; Owen, Noel L.1; Feist, William C.2, Infrared Studies of Wood Weathering. Part I: Softwoods *Society for Applied Spectroscopy*, 45 (1991) 521-714 (May 1991) , pp. 1641-1647(1997).
- [30] L. Tolvaj, O. Faix, Artificial ageing of wood monitored by DRIFT spectroscopy and CIE L*a*b* color measurements, *Holzforschung*, 49 (1995) 397-404.
- [31] M. Kishino, T. Nakano, Artificial weathering of tropical woods. Part 2: Color change, *Holzforschung*, 58 (2004) 558-565.

- [32] K.K. Pandey, Study of the effect of photo-irradiation on the surface chemistry of wood, *Polymer Degradation and Stability*, 90 (2005) 9-20.
- [33] K.K. Pandey, A Study of Chemical Structure of Soft and Hardwood and Wood Polymers by FTIR Spectroscopy, *Journal of Applied Polymer Science*, 71 (1999) 1969-1975.
- [34] R.A. Kotilainen, T.J. Toivanen, R.J. Alén, FTIR monitoring of chemical changes in softwood during heating, *Journal of Wood Chemistry and Technology*, 20 (2000) 307-320.
- [35] M.L. Nelson, R.T. O'Connor, Relation of certain infrared bands to cellulose crystallinity and crystal lattice type. Part II. A new infrared ratio for estimation of crystallinity in cellulose I and II, *J. Appl. Polym. Sci.*, 8 (1964) 1325-1341.
- [36] M. Akgül, E. Gümüşkaya, S. Korkut, Crystalline structure of heat-treated Scots pine [*Pinus sylvestris* L.] and Uludağ fir [*Abies nordmanniana* (Stev.) subsp. *bornmuelleriana* (Mattf.)] wood, *Wood Science and Technology*, 41 (2007) 281-289.
- [37] D. Fengel, G. Wegener, Lignin - Polysaccharide complexes, *Wood: Chemistry, Ultrastructure, Reactions*, (2003) 167-174.
- [38] W.C. Feist, D.N.S. Hon, Chemistry of weathering and protection, *The Chemistry of Solid Wood*, (1984) 401-451.



Fig.1 Visual appearance of tangential surfaces of birch, untreated and heat-treated at different temperatures during weathering: (a) untreated, (b) heat-treated at 195°C, (c) heat-treated at 205°C, (d) heat-treated at 215°C

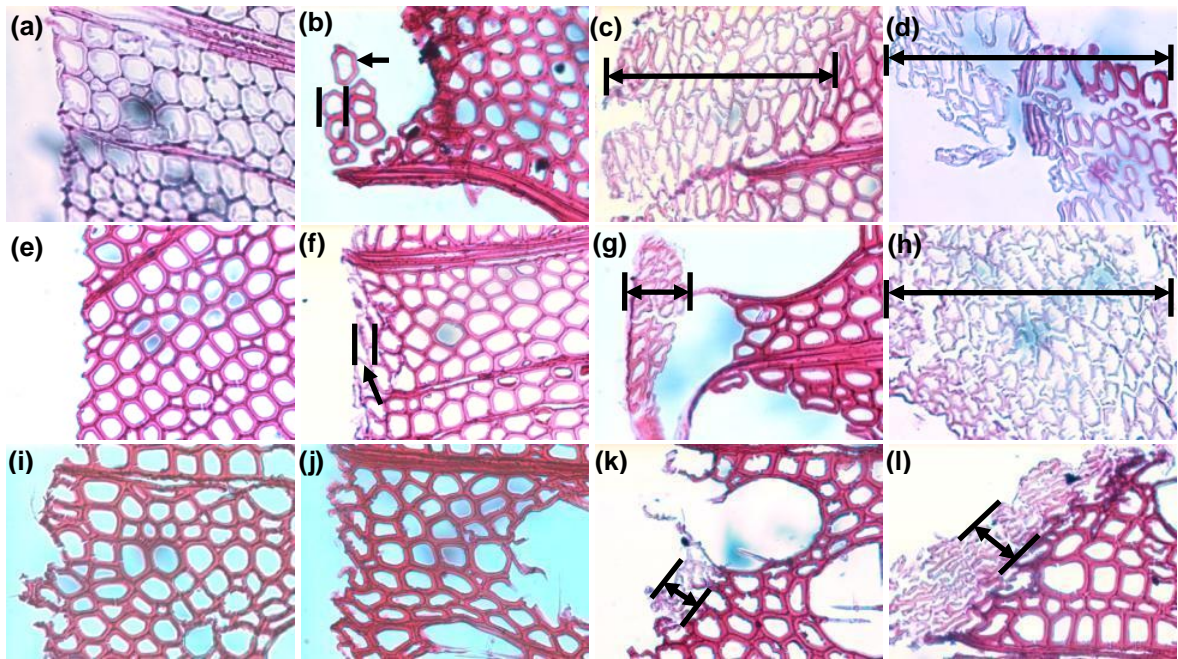


Fig. 2 Fluorescent microscope images (x50) of transverse surface of untreated birch (a-d), and heat-treated birch at 195°C (e-h), and 215°C, (i-l) after different weathering times: (a,e,i) 0h; (b,f,j) 72h; (c,g,k) 672 h; (d,h,l) 1512 h

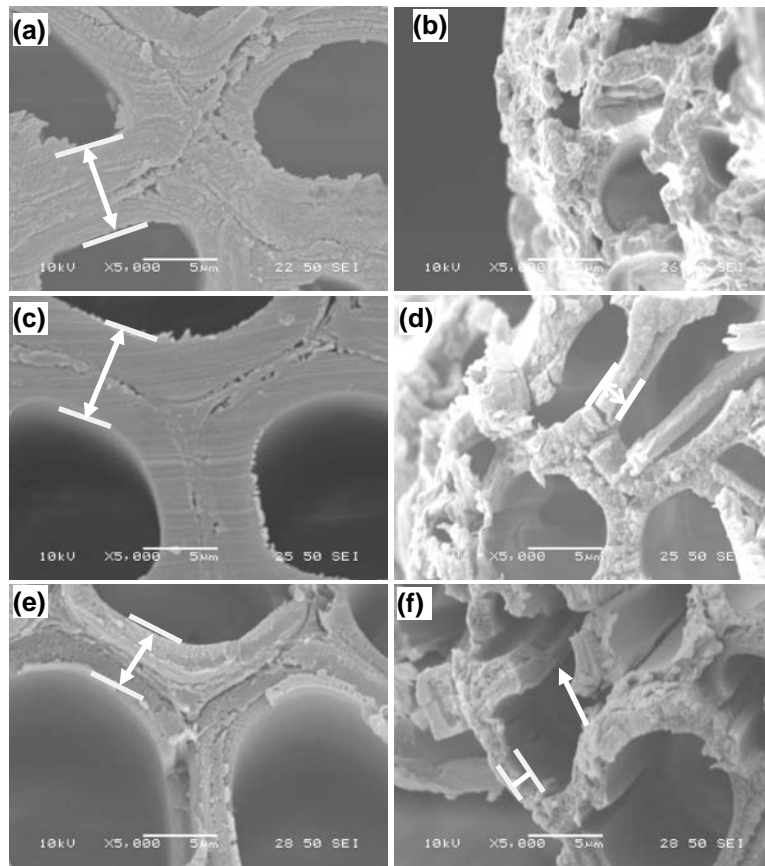


Fig. 3 SEM images ($\times 5000$) on transverse surfaces of birch specimens before and after 1512 h of artificial weathering: (a) untreated before weathering; (b) untreated after weathering; (c) heat-treated at 195°C before weathering; (d) heat-treated at 195°C after weathering; (e) heat-treated at 215°C before weathering; (f) heat-treated at 215°C after weathering

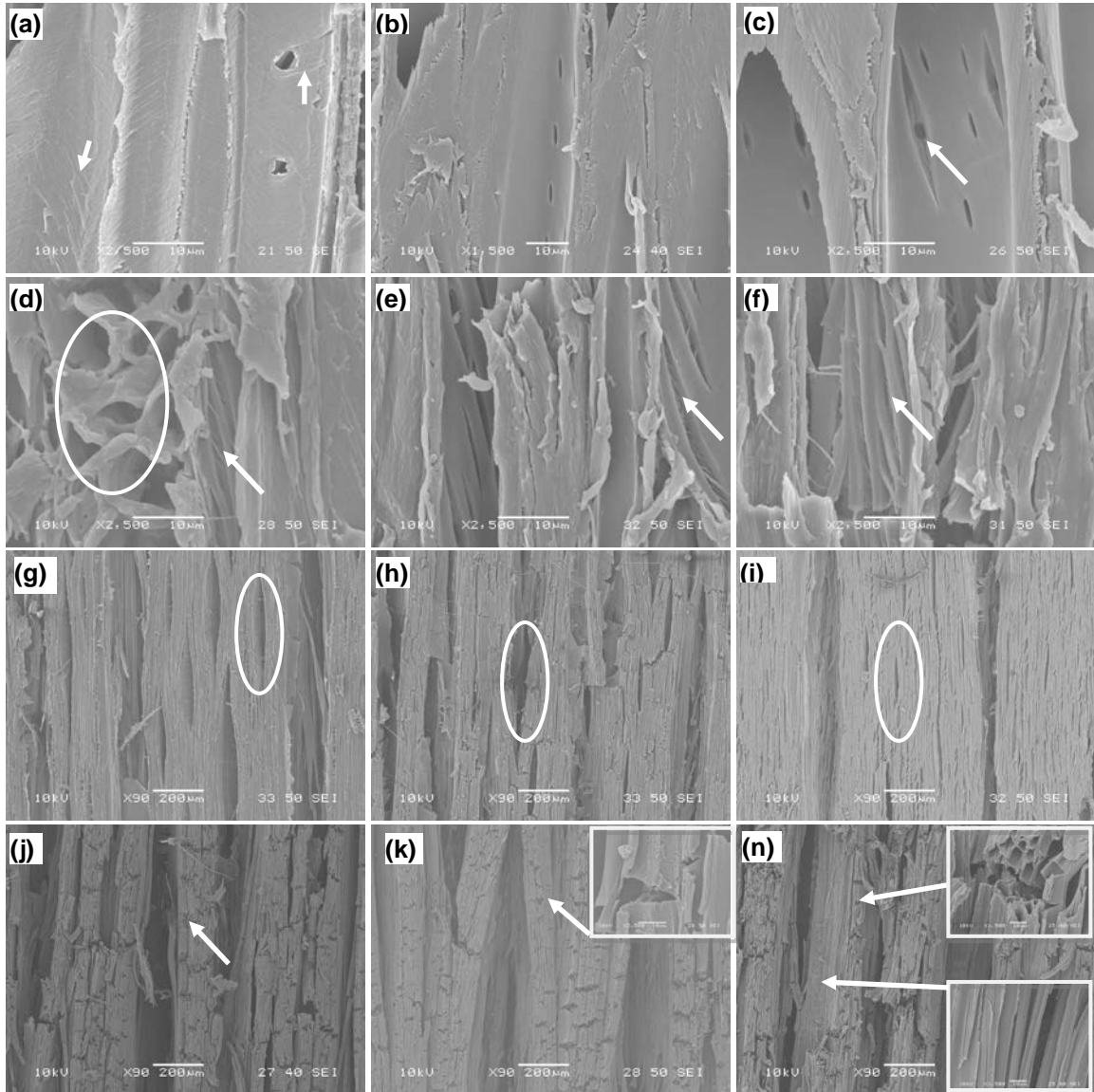


Fig. 4 SEM images on longitudinal tangential surfaces of specimens before and after artificial weathering: (a) untreated and before weathering; (b) heat-treated at 195°C and before weathering; (c) heat-treated at 215°C and before weathering; (d) untreated and after weathering of 72 h; (e) heat-treated at 195°C and after weathering of 72 h; (f) heat-treated at 215°C and after weathering of 72 h; (g) untreated and after weathering of 672 h; (h) heat-treated at 195°C and after weathering of 672 h; (i) heat-treated at 215°C and after weathering of 672 h; (j) untreated and after weathering of 1512 h; (k) heat-treated at 195°C and after weathering of 1512 h; (n) heat-treated at 215°C and after weathering of 1512 h

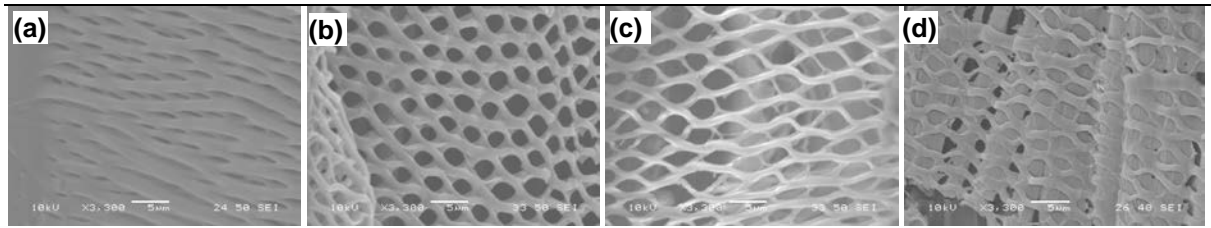


Fig. 5 SEM images of pits between fibers and vessels of birch heat-treated at 215°C and after weathering for different times: (a) before weathering; (b) 72 h, (c) 672 h, (d) 1512 h of weathering

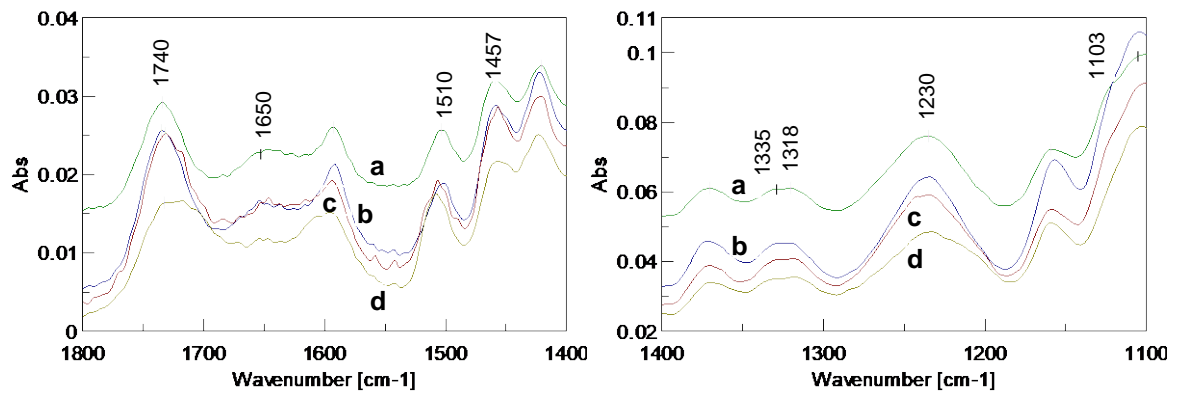


Fig. 6 FTIR spectra of birch heat-treated to different temperatures: (a) untreated; heat-treated to (b) 195°C, (c) 205°C, (d) 215°C

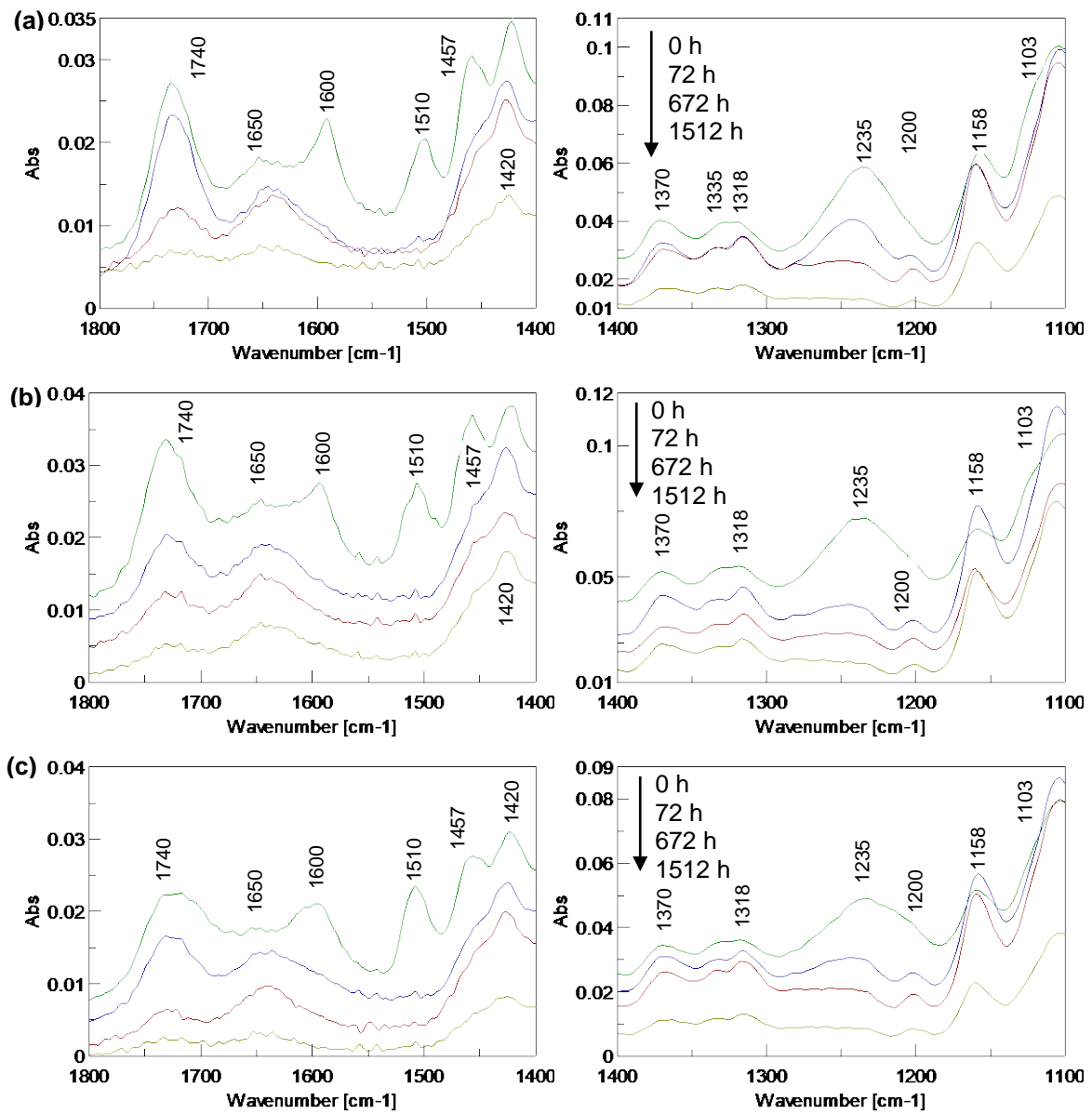


Fig. 7 FTIR spectra of heat-treated birch during artificial weathering: (a) 195°C, (b) 205°C, (c) 215°C

Erreur ! Liaison incorrecte.Erreur ! Liaison incorrecte.Erreur ! Liaison incorrecte.
(a) (b) (c)

Fig.8 (a) Ratio of band at 1740 cm^{-1} over carbohydrate band at 1370 cm^{-1} as a function of weathering time for heat-treated and untreated birch, (b) Evolution of the lignin loss as a function of weathering time, (c) Evolution of the cellulose I and amorphous cellulose content as a function of weathering time

Erreur ! Liaison incorrecte.Erreur ! Liaison incorrecte.

(a)

(b)

Fig. 9 Changes in crystallinity of heat-treated birch during artificial weathering: (a) Total crystallinity index (H_{1370}/H_{2900}), (b) Lateral order index (H_{1429}/H_{898})

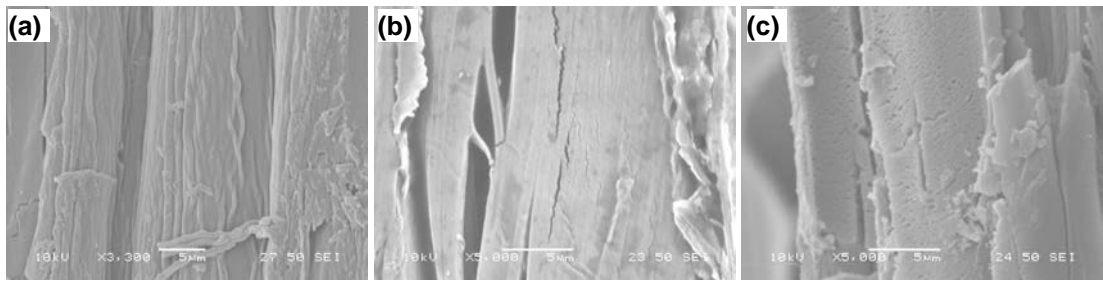


Fig. 10 Effect of weathering (1512 h) on cellulose fibrils: (a) water leaching out of by-products formed by the degradation of lignin

Table 1 Heat treatment conditions

Sample No.	Surface	Maximal temp. (°C)	Heating rate (°C/h)	Holding time (h)	Presence of humidity during heat-treatment
1	LT	untreated	-	-	-
2	LR	untreated	-	-	-
3	LT	195	15	1	Yes
4	LR	195	15	1	Yes
5	LT	205	15	1	Yes
6	LR	205	15	1	Yes
7	LT	215	15	1	Yes
8	LR	215	15	1	Yes

Table 2 Variation of the average absorbance values of untreated and heat-treated birch as a function of weathering time

Heat treatment	Weathering time (h)	Assignment						
		Hemicell+lignin	Lignin	Lignin	Lignin	Cellulose	Cellulose	Cellulose
		C=O	C=C	C=C	C-H	C-H ₂	O-H	CH ₂
		1740	1600	1510	1457	1420	1335	1318
Untreated	0	0.030	0.009	0.009	0.017	0.019	0.034	0.035
	72	0.013	0.005	0.004	0.012	0.017	0.024	0.026
	672	0.006	0.005	0.004	0.012	0.016	0.023	0.026
	1512	0.002	0.002	0.002	0.004	0.006	0.008	0.009
Heat-treated at 195°C	0	0.021	0.017	0.015	0.025	0.030	0.029	0.030
	72	0.021	0.008	0.006	0.018	0.026	0.034	0.038
	672	0.009	0.008	0.005	0.017	0.024	0.032	0.035
	1512	0.004	0.003	0.003	0.007	0.011	0.014	0.016
Heat-treated at 205°C	0	0.022	0.016	0.016	0.026	0.028	0.033	0.035
	72	0.014	0.009	0.007	0.020	0.027	0.035	0.040
	672	0.009	0.008	0.007	0.017	0.021	0.029	0.032
	1512	0.007	0.008	0.007	0.015	0.021	0.026	0.029
Heat-treated at 215°C	0	0.016	0.014	0.017	0.022	0.025	0.021	0.022
	72	0.014	0.010	0.007	0.016	0.022	0.029	0.032
	672	0.007	0.007	0.006	0.015	0.021	0.029	0.032
	1512	0.003	0.002	0.002	0.006	0.008	0.012	0.014